05,04,01,13

Propagation of spin waves in channels formed by decoration of the surfaces of yttrium-iron garnet films by thin metal areas

© V.K. Sakharov[1,2], Y.V. Khivintsev[1,2], A.S. Dzhumaliev[1], Y.V. Nikulin[1,2], M.E. Seleznev[1], Y.A. Filimonov[1,2]

[1] Saratov Branch, Kotel'nikov Institute of Radio Engineering and Electronics, Russian Academy of Sciences, Saratov, Russia
[2] Saratov National Research State University, Saratov, Russia

E-mail: valentin@sakharov.info

Received April 17, 2023
Revised April 17, 2023
Accepted May 11, 2023

Transmission of magnetostatic surface waves (MSSW) through the microchannels formed by decoration of yttrium-iron garnet (YIG) film with non-magnetic (chromium) and ferromagnetic (permalloy) metals having thickness of 30 nm was experimentally studied. MSSW losses induced by the considered metals and MSSW dispersion curves are compared with theoretical dependencies calculated taking into account the finite conductivity and magnetization of the metal layers. Possibility to reach the „antireflective" effect in the amplitude-frequency dependencies of MSSW transmission coefficient with the help of YIG film decoration with the permalloy elements was shown.

Keywords: Spin waves, yttrium-iron garnet, microantennas, decorated structures.

DOI: 10.61011/PSS.2023.07.56404.20H

1. Introduction

Development of energy-efficient devices for information storage, processing and transmission may be based on using spin waves (SW) as information carriers [1–4]. Principles of operation of such devices imply necessity for generation of SW beams and their control, which may be implemented by various methods: direct etching of film waveguides [4–6], using relief of substrates [7,8], focusing antennas and transducers of complex shape [9–12], nonuniform external fields [13–15] and decorations from ferromagnetic metals on the surface of ferrite films [16,17]. The latter method has several advantages associated with the relative simplicity of technological design, and is based on using, first of all, metallization, as SW absorber through growth of insertion losses [18] and, secondly, change of the magnetic field in the ferrite as a result of effect from the magnetic component of the decorations. The objective of this paper — is to study the mechanisms to control the dispersion and attenuation of magnetostatic surface wave (MSSW) in channels formed in films of yttrium-iron garnet (YIG) by dissipative magnetic and non-magnetic loads, such as films of permalloy (Py) and chrome (Cr).

Please note that metallization of YIG with a layer of Py means formation of a bilayer magnetic structure, spectra of MSSW in which were studied in detail neglecting the layers conductivity [19–22]. In these researches, the main attention was paid to features in dispersion formation for so called internal MSSW, which in the short-wavelength range has the maximum amplitude at the interface.

2. Studied structures, experiment and calculation techniques

Microstructures studied in the paper were made on the basis of a YIG film with a thickness $d = 6.5\,\mu$m and magnetization $4\pi M = 1830$ G, grown by liquid-phase epitaxy on the substrate of gadolinium-gallium garnet (GGG). On the surface of this film, copper microantennas (MA) with contact pads and areas (decorations) from Cr and Py were formed — see Fig. 1. Four technological stages were fulfilled in step-by-step order for every material: film deposition by DC magnetron sputtering; photolithography — formation of a pattern from polymer (photoresist) on the surface of this film; ion etching of metal film areas not protected with photoresist; and sample cleaning from photoresist remains. All structures were made on the same YIG/GGG plate within the same technological cycle, providing the identity of decoration and antenna thicknesses for all structures. At the same time, the described technology results in YIG etched to a small thickness d_{et} together with the metal areas that are not protected by photoresist. In particular, this is true for the stage of copper antenna fabrication, since the copper layer thickness for them was ≈ 850 nm, and when the required copper areas were etched in the entire sample area, the excessive time was kept, so the YIG film overetching was $d_{et} \approx 15-20$ nm. Thickness of decorations from Cr and Py was $\delta = 30$ nm, and for them YIG film overetching was minor ($d_{et} \approx 1-5$ nm).

Besides, structures were also made on the sample to measure the specific resistance ρ of the used metals, which

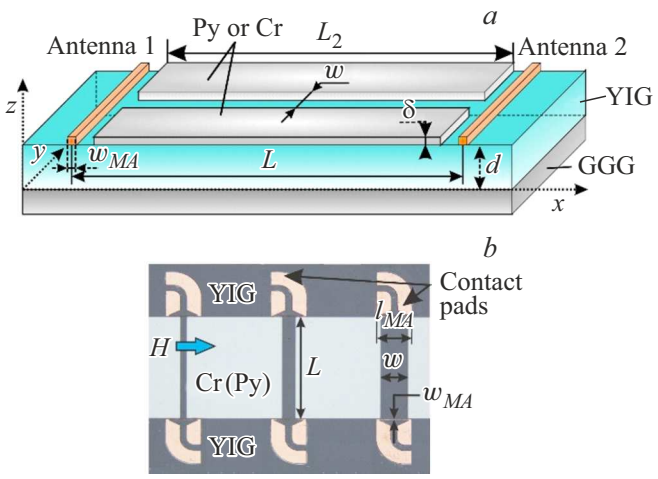

Figure 1. Schematic image (a) and microphotography (b) of some considered structures with indication of geometric parameters.

was defined using a the four-probe method and amounted to: $\rho(\mathrm{Cr}) = 0.61$ and $\rho(\mathrm{Py}) = 0.73\,\mu\Omega\cdot\mathrm{m}$. Therefore, the difference in the resistance of decorations materials was 16%. The skin layer depth l_{sk} for typical frequencies f of MSSW excitation in YIG ($f = 2{-}7\,\mathrm{GHz}$) in this case is $l_{sk}(\mathrm{Cr}) \approx 6.8\,\mu\mathrm{m}$; $l_{sk}(\mathrm{Py}) \approx 0.3\,\mu\mathrm{m}$.

Please note that chrome is antiferromagnetic. Antiferromagnetic order and proximity to the Neel temperature (38°C) causes almost the absence of external fields, therefore, its magnetic properties may be neglected.

The length of the used MA was $l_{MA} = 250\,\mu\mathrm{m}$, the width — $w_{MA} = 4\,\mu\mathrm{m}$, which provided excitation of MSSW with wave numbers $k \leq \pi/w_{MA} \approx 8\cdot 10^3$ rad/cm. Two sets of the structures were considered — for the first set, the distance between the exciting and receiving MA was $L = 820\,\mu\mathrm{m}$, for the second one — $L = 220\,\mu\mathrm{m}$. The studied structures have the channel width w from the following set 12, 24, 50, 100 and $200\,\mu\mathrm{m}$, besides, a structure without decorations („free“ YIG film) and a fully metallized YIG surface between input and output MA ($w = 0$) were studied. External magnetic field H was applied along MA, which corresponds to the case of Damon–Eshbach [23] MSSW.

The measurement method was similar to the method described in [17], except for the fact that prior to applying the signal to the network analyzer, a pre-amplifier was not used. Power of the signal applied to the input antenna was $-40\,\mathrm{dBm}$ (at fields $H = 120{-}810\,\mathrm{Oe}$) and $-25\,\mathrm{dBm}$ (at fields $H > 810\,\mathrm{Oe}$), which was less than the threshold of parametric instability.

To interpret the results of measurements for the structures with Py, calculation of equilibrium distribution of the field and magnetization in YIG film was carried out using OOMMF 1.2b0 software [24]. Material parameters were chosen as corresponding to experimental samples: exchange stiffness — $A_{ex}(\mathrm{Py}) = 11.5\cdot 10^{-7}\,\mathrm{erg/cm}$, $A_{ex}(\mathrm{YIG}) = 3.13\cdot 10^{-7}\,\mathrm{erg/cm}$; effective magnetization — $4\pi M(\mathrm{Py}) = 9.2\,\mathrm{kG}$, $4\pi M(\mathrm{YIG}) = 1.83\,\mathrm{kG}$.

We will calculate dispersion curves $k'(f)$ of MSSW and losses (which we will express in the imaginary part of the wave number $k = k' - ik''$) for YIG/Cr and YIG/Py structures with account of conductivity and magnetization of metal layers, but not taking into account the exchange interaction, based on the equations of Landau–Lifshitz and Maxwell, according to the method similar to papers [17,25,26]. One can also calculate dispersion curve $k'(f)$ of internal MSSW using the method developed for nonuniform films [27], having set the film profile from two ferromagnetic layers corresponding to YIG and Py, without account of conductivity, losses and exchange interaction. In the calculations, we will assume the FMR line width ΔH as equal to typical values for YIG — $\Delta H = 0.4\,\mathrm{Oe}$, and thicknesses of metal layers will be taken as $\delta(\mathrm{Py}) = 25\,\mathrm{nm}$ and $\delta(\mathrm{Cr}) = 35\,\mathrm{nm}$, since the best matching with the experimental data discussed below is achieved for these values.

3. Results and discussion

3.1. Expected impact of chrome and permalloy layers

For the selected values of thickness of metal films $\delta = 30\,\mathrm{nm}$ and depth $l_{sk} \approx 6.8\,\mu\mathrm{m}$, the value of parameter $G = \delta/(kl_{sk}^2)$, characterizing impact of metal at properties of MSSW [18], is $G \leq /(\pi l_{sk}^2) \approx 0.3$. In this case, the impact of conductivity of the metal layers results in introducing additional ohmic losses (losses due to spin pumping, as a rule do not exceed magnetic losses in YIG [28] and are not considered here) for transmission of MSSW [18] without a transition to the second branch of dispersion with large short-wavelength border [29]. Close conductivity of Cr and Py makes it possible to define impact of magnetic component in Py at characteristics of propagation of MSSW from comparison of measurement results. Besides, it is possible to expect that the magnetic subsystem of areas from Py will result in two main features. First, Py layer leads to the formation of a bilayer magnetic film, therefore, MSSW with the maximum of amplitude near the interface with Py film must be converted to „internal MSSW“ [19–22]. Second, demagnetizing fields from the edges of channels in metallization from Py will modify the internal field in the underlying YIG layer. Let us consider both of these effects in more detail.

For the case of free film, the range of MSSW [23] existence is limited by frequencies $f_0 = \gamma\sqrt{H(H + 4\pi M)}$ and $f_S = \gamma(H + 4\pi M/2)$, where γ — gyromagnetic ratio shown by dot-and-dash vertical lines in Fig. 2. Accounting of impact of the finite conductivity of metallization from Cr results in the calculated dispersion of MSSW, weakly different from the curve for the free YIG film (see curve *1* in Fig. 2, *a*). At the same time, the presence of Cr introduces

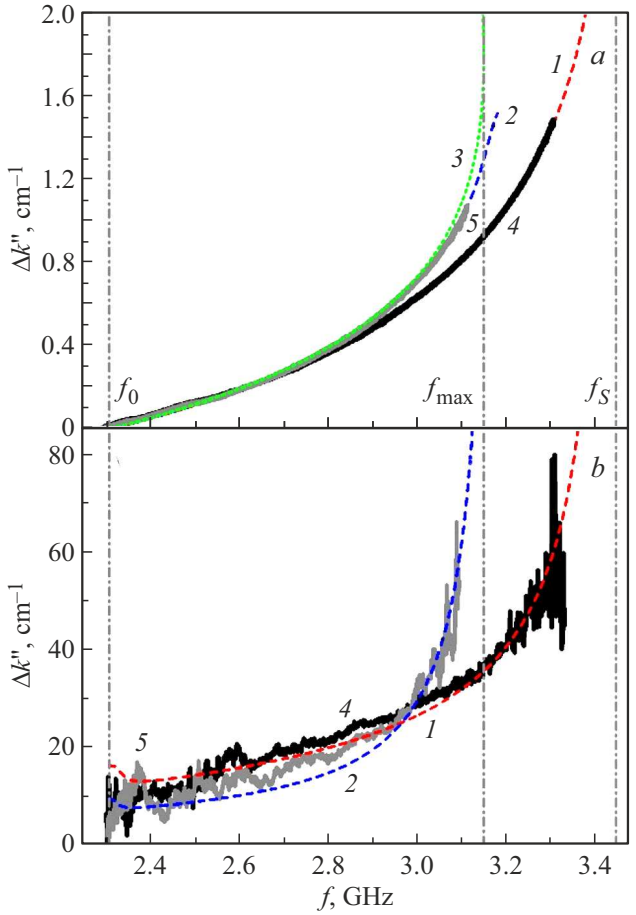

Figure 2. Dispersion curves (a) and contribution of metallization to the spatial decrement (b) for MSSW in YIG/Cr and YIG/Py at $H = 316$ Oe. Curves *1* — calculated dispersion and losses for YIG/Cr; curves *2* — for YIG/Py; curve *3* — dispersion for YIG/Py, calculated according to [27]; curves *4* and *5* — experimental dispersions (a) and losses (b) for metallization from Cr and Py, respectively.

more ohmic losses for MSSW $\Delta k''(f)$ relative to losses in the free YIG film. Besides, $\Delta k''$ grows as MSSW shortens, considerably increasing losses near the short-wavelength border (compare curve *1* in Fig. 2, b). In the experiment, it may manifest itself in narrowing of the MSSW transmission band due to the strong suppression of the wave in the short-wavelength part of the spectrum.

In the case of YIG/Py, the dependence $k'(f)$ (curve *2* in Fig. 2, a) changes considerably compared to the free YIG film. Calculation according to [27] (curve *3* in Fig. 2, a) shows the formation of a maximum at frequency $f_{\max} \approx 3.15$ GHz below the short-wavelength border of MSSW f_S. At the same time, losses in YIG/Py $\Delta k''(f)$ additional to losses in the free YIG film (curve *2* in Fig. 2, b) turn out to be less than ones for the case of YIG/Cr up to the frequency ≈ 2.96 GHz, since $\rho(\text{Py}) < \rho(\text{Cr})$ and $\delta(\text{Py}) < \delta(\text{Cr})$, but at higher frequencies, they considerably exceed the losses in YIG/Cr due to additional magnetic losses from Py, as a magnet. Therefore, in the experiment, the MSSW transmission band in YIG/Py must narrow down both compared to the free YIG film and YIG/Cr structure.

Now let us consider how demagnetization fields from areas of Py impact on the distribution of internal field in the YIG layer. One can see that in the area of the Py decoration edge, the internal field becomes substantially nonuniform (Fig. 3). Width of the highest nonuniformity along axis x stretches for $\approx 5\,\mu$m to both sides away from the edge of the Py area, and along axis y, it reaches location of antennas (Fig. 3). Field distribution under the channel reminds the distribution between the electromagnet poles — reaches the maximum values near the border of the decorations and gradually reduces to the center of the channel. Besides, the internal field under the channels has higher values compared to the field under antennas, and is similar to distribution of field of a billow type considered in [15]. Therefore, the wave that entered the channel will be transformed according to the Schlomann's mechanism [30] as a result of gradual field change to a longer-wave MSSW, having higher group velocity, and, accordingly, smaller propagation losses. Nevertheless, at $w = 50-200\,\mu$m, the change of the field

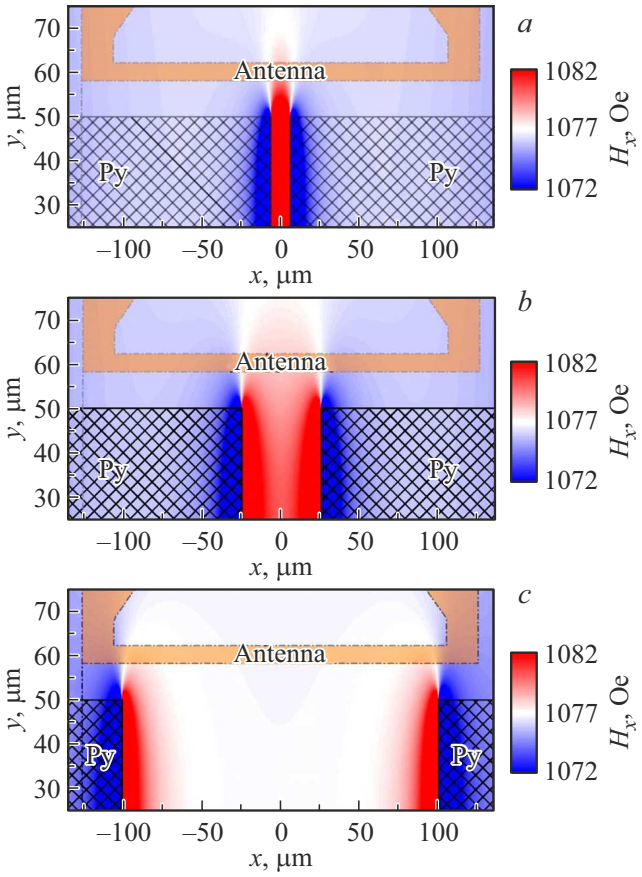

Figure 3. Distribution of x-component of the internal field in the near-surface layer of YIG film with decorations from Py with width of channel $12\,\mu$m (a), $50\,\mu$m (b) and $200\,\mu$m (c) at external applied field $H = 1077$ Oe. Shaded regions denote areas coated by Py, area with semi-transparent fill denotes input antenna location.

from the input antenna to the output one along the channel axis is not more than 3–4 Oe. Therefore, in this case, the transformation effect has an insignificant value.

The channeling effect should be much more significant. It consists in the following. The area of nonuniformity along the channel borders divides the incident MSSW into three components. Two of them transform into the internal MSSW under areas metallized by Py, and can not propagate in the frequency range $[f_{\max}, f_S]$ (see Fig. 2), and the third part of MSSW gets in the channel area. In addition, the area of nonuniformity along the channel borders and absence of the allowed states for $[f_{\max}, f_S]$ prevents diffraction spreading of the MSSW that entered the channel and forms a directed wave beam.

Please note that propagation of MSSW from the input antenna occurs within the limits of the cut-off angles φ_s (between the normal line to the antenna and the direction, along which MSSW can still propagate), defined according to the expression [23]:

$$\varphi_s = 90^\circ - \operatorname{atan}\sqrt{\frac{H}{4\pi M}}.$$

For field $H = 316$ Oe, the cut-off angle is $\varphi_s \approx 67^\circ$, for $H = 1077$ Oe — $\varphi_s \approx 53^\circ$, and for $H = 1573$ Oe — $\varphi_s \approx 47^\circ$. Therefore, the diffraction spreading of MSSW from the input antenna in absence of the channels is quite significant in the considered range of fields.

3.2. MSSW transmission in metallized structures

From comparison of amplitude-frequency characteristic (AFC) of the MSSW transmission coefficient $S_{12}(f)$ for the free YIG film and the YIG film metallized by permalloy or chrome (Fig. 4), several features may be identified. First of all, the fully metallized YIG surface results in deterioration of MSSW transmission compared to the free YIG film as a result of losses introduced by conductivity of Cr and Py [17]. By difference of curves $S_{12}^M(f)$ and $S_{12}^0(f)$, corresponding to the case of metallized YIG film and YIG film without metal, respectively, it is possible to determine the contribution of metallization to decrement k'', based on ratio

$$\Delta k'' = \frac{S_{12}^M(f) - S_{12}^0(f)}{8.68 \cdot L} = \frac{\Delta S_{12}[dB]}{8.68 \cdot L}.$$

Experimental curves $\Delta k''(f)$ obtained in such manner for the field 316 Oe (Fig. 2, *b*) have a good agreement with the theoretical curves for $\delta(\text{Py}) = 25$ nm and $\delta(\text{Cr}) = 35$ nm. Besides, for the same thicknesses of Py and Cr, the experimental dispersion curves $k'(f)$ obtained from the phase incursion also demonstrate good agreement with the theoretical curves (Fig. 2, *a*).

Please note that transmission region with the width of ≈ 20–80 MHz below the frequency f_0 is due to magnetostatic backward volume waves (MSBVW).

From Fig. 4, one can also identify the difference of $S_{12}(f)$ curves for YIG/Cr and YIG/Py in the short wavelength

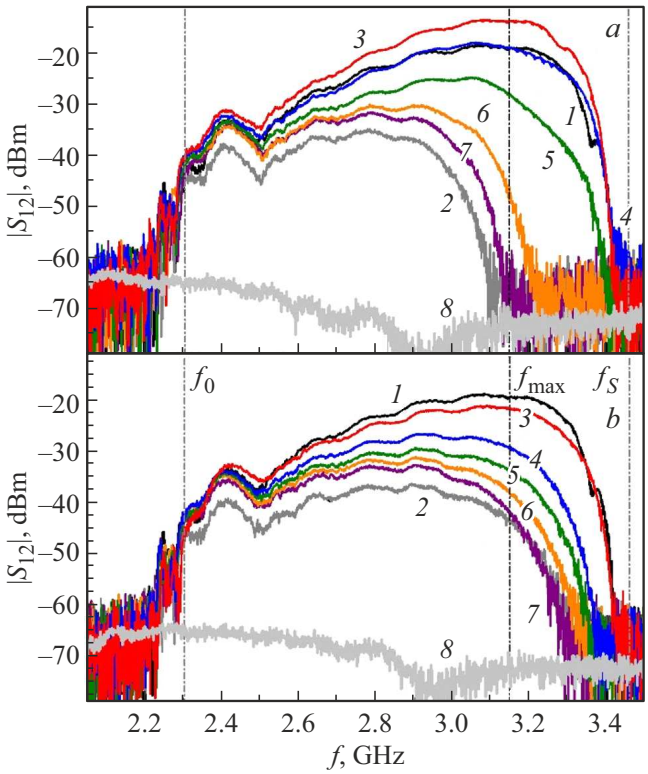

Figure 4. Amplitude-frequency characteristics of the transmission coefficient in YIG film without metallization (curve *1*), fully metallized YIG (curve *2*); structures with width of channel $w = 200\,\mu$m (curve *3*), $100\,\mu$m (curve *4*), $50\,\mu$m (curve *5*), $24\,\mu$m (curve *6*), $12\,\mu$m (curve *7*) in decorations from Py (*a*) and Cr (*b*) at the field $H = 316$ Oe. Channel length $L_2 = 800\,\mu$m. Frequencies f_0, $f_{\max}$, f_S correspond to Fig. 2. Cross-talk level is indicated by curve *8*.

region $[f_{\max}, f_S]$. As it was noted in section 3.1, for the YIG/Py structure, the dispersion of MSSW in YIG layer is limited by the range of frequencies $[f_0, f_{\max}]$, where $f_{\max} < f_S$. As a result, the width of the MSSW transmission band in YIG/Py is less than the corresponding band both in the free YIG film and in the YIG/Cr structure. However, the difference in the width of transmission band for YIG/Py and YIG/Cr reduced with growth of applied field from ≈ 560 MHz at $H \approx 120$ Oe practically to zero for $H \approx 550$ Oe (for $L = 820\,\mu$m) or $H \approx 1570$ Oe (for $L = 220\,\mu$m). With further growth of the field, the transmission band for metallization from Py and Cr remained of approximately the same width. This is because the increase of the applied field is accompanied by the growth of losses caused by reduction of group velocity of MSSW, which, in its turn, is caused by reduction of the range $[f_0, f_S]$ and the corresponding „flattening“ of dispersion. At the same time, the range of wave numbers recorded in the experiment reduces, and when it reaches the region, where the dispersion characteristics for YIG/Py and YIG/Cr weakly differ from each other, the width of the transmission bands equalizes.

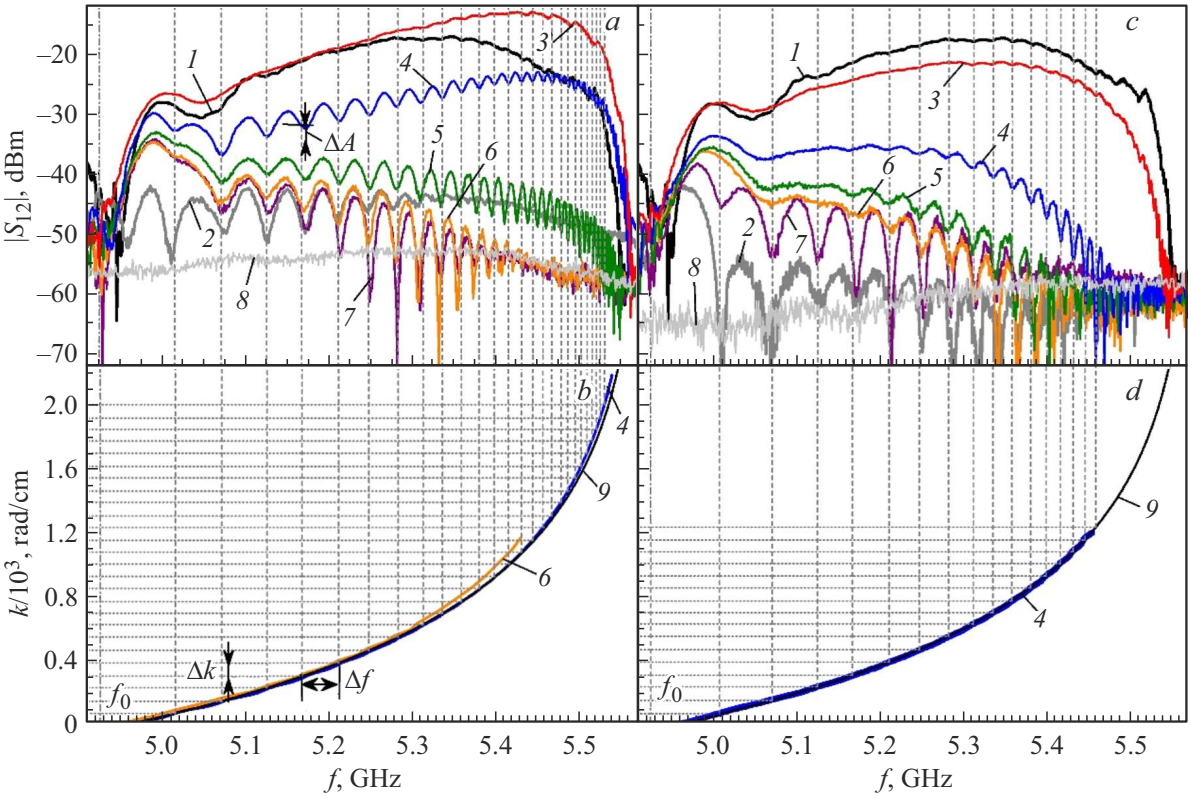

Figure 5. Amplitude-frequency characteristics (a, c) and dispersion curves (b, d) for free film (curves *1*) and structures based on decorations from Py (a, b) and Cr (c, d) with channel length $L_2 = 800\,\mu$m and width $w = 0\,\mu$m (curves *2*), $w = 200\,\mu$m (curves *3*), $w = 100\,\mu$m (curves *4*), $w = 50\,\mu$m (curves *5*), $w = 24\,\mu$m (curves *6*), $w = 12\,\mu$m (curves *7*). Curve *8* indicates the cross-talk level for $w = 50\,\mu$m. External field $H = 1077$ Oe. Dashed lines show the positions of resonances for $w = 50\,\mu$m (a, b) and $w = 100\,\mu$m (c, d).

3.3. MSSW transmission in structures with channels

Let us analyze the results measured for the structures with channels, and let us start with the consideration of structures with the channel length $L_2 = 800\,\mu$m. In Fig. 4, there are dependencies $S_{12}(f)$ for structures with various width of the channel in decorations from Py and Cr at the applied field $H = 316$ Oe, and in Fig. 5 — at field $H = 1077$ Oe, respectively.

When there is a channel in metallization, a part of the wave beam from the exciting MA gets into the channel, as a result all $S_{12}(f)$ curves turned out to be located between the curves corresponding to the extreme cases of fully metallized and free surface. The exception is the case of channel in Py with width $w = 200\,\mu$m, for which $S_{12}(f)$ curves demonstrate smaller or equal transmission losses for MSSW compared to the free YIG film. The fact that this effect only happens for metallization from Py, indicates there is effect of the magnetic system of decorations. As it was considered in section 3.1, this becomes possible as a result of the channeling effect caused by features of the dispersion characteristic of MSSW in YIG/Py and nonuniformity of the field at the border of the channel and decorations. To a smaller extent the transmission improvement is due to the effect of wave length transformation related to change of the internal field along the channel axis from the input to the output antenna. Depending on the width of the channel, there will be a different ratio between the components of the incident signal (two components are internal MSSWs in decorated YIG/Py areas at both sides from the channel, and the third component is MSSW in the channel area), since the antenna length is fixed $l_{MA} = 250\,\mu$m. At $w = 200\,\mu$m, most of the input signal enters the channel, and due to the considered transformation and channeling effects, the transmission turns out to be better than MSSW transmission in the free film. With reduction of the channel width, the contribution of the signal passing through the channel reduces, since in the experiment, the antenna aperture was fixed for all structures with different channel width, which is reflected in AFC.

Experimental dispersion characteristics (Fig. 5, *b, d* and Fig. 6, *b, d*), obtained from the measurements for $w = 12-200\,\mu$m, correspond to the dispersion curves for free YIG film, which confirms transmission of MSSW signal mostly through the channel.

Comparison of $S_{12}(f)$ curves for the channels from Cr and Py (Fig. 4, *a* and *b*; Fig. 5, *a* and *c*) shows that the short-wavelength region of AFC in the structures from

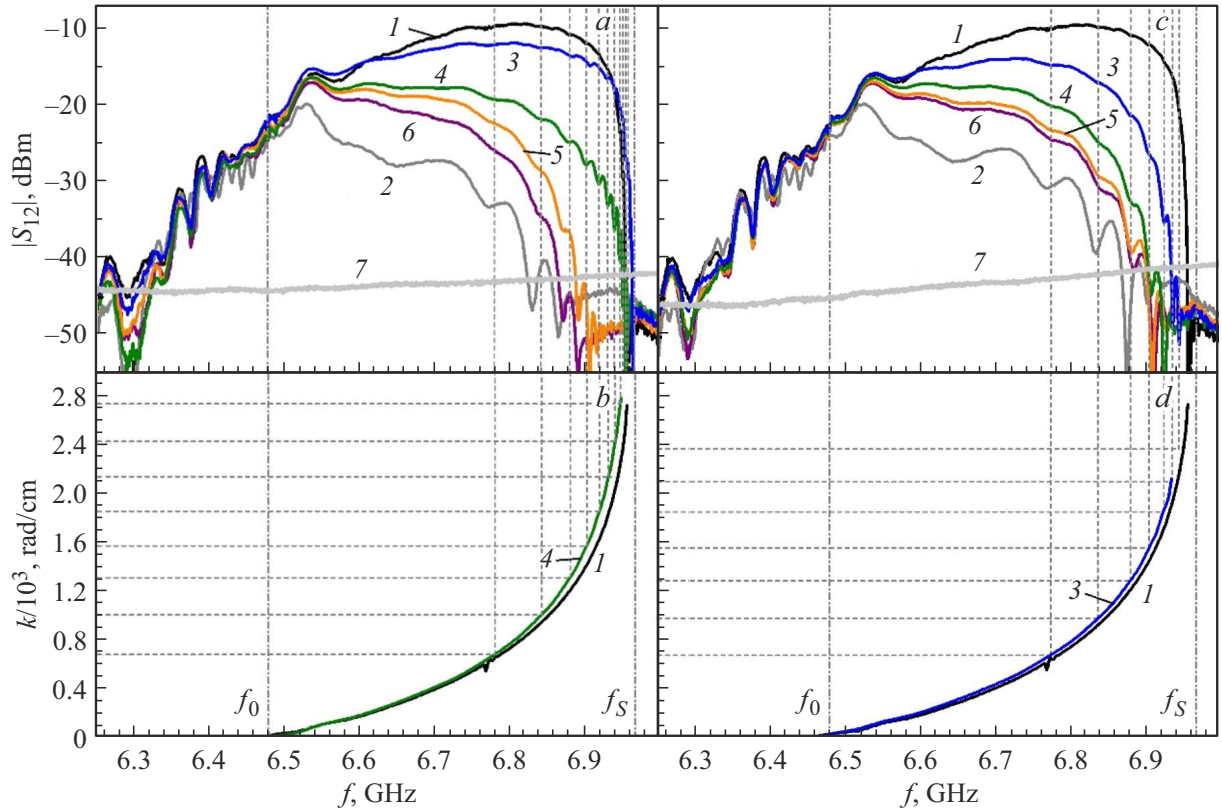

Figure 6. Amplitude-frequency characteristics (a, c) and dispersion curves (b, d) for free YIG film (curves *1*) and structures based on the decorations from Py (a, b) and Cr (c, d) with channel length $L_2 = 200\,\mu$m and width $w = 0\,\mu$m (curves *2*), $w = 100\,\mu$m (curves *3*), $w = 50\,\mu$m (curves *4*), $w = 24\,\mu$m (curves *5*), $w = 12\,\mu$m (curves *6*). Curve *7* shows the cross-talk level for metallized YIG. External field $H = 1573$ Oe. Dashed lines show the positions of resonances for $w = 100\,\mu$m, dot-and-dash lines — the position of border frequencies of MSSW.

Py at $w > 50\,\mu$m demonstrates better transmission due to described transformation and channeling effects. At the same time, for $w = 12$ and $24\,\mu$m, transmission in the structures from Py turns out to be worse than in the corresponding structures from Cr, which happens under the effect of two reasons. First, it is the effect of absence of allowed states in $[f_{\max}, f_S]$ (see Fig. 2) for the internal MSSW in YIG/Py structure, which causes different (from YIG/Cr) attenuation under metallized areas exactly in the high frequency part of the transmission band. Secondly, areas of strong nonuniformity of fields near the areas of YIG film coated by Py, occupy substantial part of channels at $w = 12$ and $24\,\mu$m.

With the growth of field (at $H \geq 550$ Oe), formation of oscillations was observed in $S_{12}(f)$ curves for the structures from both Py and Cr, including fully metallized YIG surface $(w = 0)$ — see Fig. 5. In addition, „depth“ of these oscillations ΔA grows with reduction of w. Frequencies of the oscillations in AFC, as it follows from experimental dispersion characteristics (Fig. 5, *b, d*), correspond to the gradual change of wave numbers by $\Delta k_1 \approx 76.9 \pm 0.5$ rad/cm between neighboring dips, which implies the spatial size $2\pi/\Delta k_1 \approx 817.4 \pm 4.8\,\mu$m that is close to the distance between the exciting and receiving antennas. Tracking of the level of direct electromagnetic cross-talk S_{12}^{CrT} between the input and output antennas shows nonmonotonic growth of S_{12}^{CrT} with the frequency increase (compare curves 8 in Fig. 4 and 5). At the same time with the field growth, the maximum values of MSSW transmission coefficients decrease. As a result of reduction in signal-to-noise ratio, the effect of their interference increases, which manifests itself in the form of oscillations in AFC of the transmission coefficient. Therefore, the mentioned oscillations dramatically differ from the resonance features observed in [17]. It is possible that absence of features described in [17] in this experiment is related to much thinner layers of decorating metal.

Let us proceed to consider transmission characteristics in the structures with channel length $L_2 = 200\,\mu$m. The example of AFC and dispersion characteristics for the considered structures from both Py and Cr at field $H = 1573$ Oe is shown in Fig. 6. As a result of smaller length of the channel, $S_{12}(f)$ dependencies demonstrate better transmission both in the MSSW band, and in the frequency range $f < f_0$, corresponding to MSBVW. Oscillations in AFC for the frequencies $f < f_0$ are due to multimode property of MSBVW.

As for case $L_2 = 800\,\mu$m, at $L_2 = 200\,\mu$m, oscillations are formed in AFC of MSSW due to interference with cross-talk. However, because of lower attenuation at such distances, interference becomes possible at fields $H \geq 1077$ Oe (for fully metallized YIG films), and the oscillations as such are less expressed in „amplitude“. The interval in wave numbers between adjacent dips is $\Delta k_2 \approx 287.5 \pm 6.4$ rad/cm, which corresponds to the spatial size $2\pi/\Delta k_2 \approx 218.6 \pm 4.9\,\mu$m in accordance with the reduced distance between antennas.

4. Conclusion

In this work, the propagation of MSSW in YIG films decorated by films of permalloy and chrome is studied. It is shown that magnetic component of metallization has significant influence on AFC of transmission coefficient and dispersion of MSSW due to transformation of MSSW in YIG to the internal MSSW under Py layer and formation of nonuniform magnetic field in the area of the channel in decorations. It was found that in decorations from magnetic metal the transmission can be improved compared to the case of free YIG film and structures decorated with non-magnetic metal, due to channeling effect caused by change of MSSW dispersion and formation of nonuniform magnetic field inside YIG due to magnetic properties of the metal.

Funding

The research was carried out as part of project № 22-22-00563 of the Russian Science Foundation.

Conflict of interest

The authors declare that they have no conflict of interest.

References

[1] V.V. Kruglyak, S.O. Demokritov, D. Grundler. J. Phys. D **43**, 264001 (2010).
[2] A.A. Serga, A.V. Chumak, B. Hillebrands. J. Phys. D **43**, 264002 (2010).
[3] S.A. Nikitov, D.V. Kalyabin, I.V. Lisenkov, A.N. Slavin, Yu.N. Barabanenkov, S.A. Osokin, A.V. Sadovnikov, E.N. Beginin, M.A. Morozova, Yu.P. Sharaevskiy, Yu.A. Filimonov, Yu.V. Khivintsev, S.L. Vysotsky, V.K. Sakharov, E.S. Pavlov. UFN, **185** (1099) (2015). (in Russian).
[4] A. Kozhevnikov, F. Gertz, G. Dudko, Y. Filimonov, A. Khitun. Appl. Phys. Lett. **106**, 142409 (2015).
[5] Y.V. Khivintsev, V.K. Sakharov, A.V. Kozhevnikov, G.M. Dudko, Y.A. Filimonov, A. Khitun. JMMM **545**, 168754 (2022).
[6] C.S. Davies, A.V. Sadovnikov, S.V. Grishin, Y.P. Sharaevsky, S.A. Nikitov, V.V. Kruglyak. IEEE Trans. Magn. **51**, 3401904 (2015).
[7] E.N. Beginin, A.V. Sadovnikov, A.Y. Sharaevskaya, A.I. Stognij, S.A. Nikitov. Appl. Phys. Lett. **112**, 122404 (2018).
[8] V.K. Sakharov, E.N. Beginin, Y.V. Khivintsev, A.V. Sadovnikov, A.I. Stognij, Y.A. Filimonov, S.A. Nikitov. Appl. Phys. Lett. **117**, 022403 (2020).
[9] A. Papp, W. Porod, A.I. Csurgay, G. Csaba. Sci. Rep. **7**, 9245 (2017).
[10] A.V. Vashkovskiy, K.V. Grechushkin, A.V. Stalmakhov, V.A. Tyulyukin. RE **31**, 838 (1986). (in Russian).
[11] R. Gieniusz, P. Gruszecki, M. Krawczyk, U. Guzowska, A. Stognij, A. Maziewski. Sci. Rep. **7**, 8771 (2017).
[12] G.M. Dudko, A.V. Kozhevnikov, V.K. Sakharov, A.V. Stalmakhov, Yu.A. Filimonov, Yu.V. Khivintsev. Izv. Saratovskogo gos. un-ta. Ser.: fizika **18**, 92 (2018). (in Russian).
[13] A.Yu. Annenkov, S.V. Gerus, S.I. Kovalev. ZhTF **74**, 98 (2004). (in Russian).
[14] D.D. Stancil, F.R. Morgenthaler. J. Appl. Phys. **54**, 1613 (1983).
[15] V.I. Zhubkov, V.I. Shcheglov. RE **46**, *9*, 1121 (2001). (in Russian).
[16] G.A. Vugalter, A.G. Korovin. J. Phys. D **31**, 1309 (1998).
[17] Yu.V. Khivintsev, G.M. Dudko, V.K. Sakharov, Yu.V. Nikulin, Yu.A. Filimonov. FTT **61**, 1664 (2019). (in Russian).
[18] A.G. Veselov, S.L. Vysotsky, G.T. Kazakov, A.G. Sukharevy, Yu.A. Filimonov. RE **39**, 2067 (1994). (in Russian).
[19] R.E. Camley, A.A. Maradudin. Solid State Commun. **41**, *8*, 585 (1982).
[20] V.I. Zubkov, V.A. Epanechnikov. Pis'ma v ZhTF **11**, *23*, 1419 (1985). (in Russian).
[21] V.I. Zubkov, E.G. Lokk, B.P. Nam, A.S. Khe, V.I. Scheglov. ZhTF **59**, *12*, 115 (1989). (in Russian).
[22] Yu.A. Filimonov, I.V. Shein. ZhTF **62**, *1*, 187 (1992). (in Russian).
[23] R.W. Damon, J.R. Eshbach. J. Phys.Chem. Solids **19**, 308 (1961).
[24] M.J. Donahue,D.G. Porter. Interagency Report **NISTIR 6376**. National Institute of Standards and Technology, Gaithersburg, MD (1999).
[25] Yu.A. Filimonov, Yu.V. Khivintsev. RE **47**, 1002 (2002). (in Russian).
[26] V.I. Zubkov, V.A. Epanechnikov, V.I. Scheglov. RE **52**, 192 (2007). (in Russian).
[27] R.A. Gallardo, P. Alvarado-Seguel, T. Schneider, C. Gonzalez-Fuentes, A. Roldán-Molina, K. Lenz, J. Lindner, P. Landeros. New J. Phys. **21**, 033026 (2019).
[28] S.M. Rezende, R.L. Rodriguez-Suarez, M.M. Soares, L.H. Vilela-Leã o, D. Ley Domínguez, A. Azevedo. Appl. Phys. Lett. **102**, 012402 (2013).
[29] S.R. Seshadri. Proc. IEEE **58**, *3*, 506–507 (1970).
[30] E. Schlomann. J. Appl. Phys. **35**, 159 (1964).

Translated by Ego Translating